RJC

RASĀYAN *J. Chem.*
Vol. 15 | No. 3 |1678-1685| July - September | 2022
ISSN: 0974-1496 | e-ISSN: 0976-0083 | CODEN: RJCABP
http://www.rasayanjournal.com
http://www.rasayanjournal.co.in

THE SYNTHESIS OF METHYLAMMONIUM LEAD IODIDE ON MESOPORE TiO_2 THIN FILM APPLYING OSTWALD RIPENING PROCESS UNDER AMBIENT CONDITION

C. Kusumawardani✉ and J. Ikhsan
Department of Chemistry, Faculty of Mathematics and Natural Sciences, Universitas Negeri Yogyakarta, 55283, Indonesia
✉Corresponding Author: cahyorini.k@uny.ac.id

ABSTRACT
Organometallic halide-based perovskite solar cells have played a significant role in the development of photovoltaic technology. The synthesis of the perovskite usually needs specific atmospheres, especially controlled humidity. Here, we demonstrate the synthesis of compact methylammonium lead iodide perovskite ($MAPbI_3$) on TiO_2 under ambient conditions through one and two-step spin-coating deposition methods, which both resulted in an unconverted PbI_2 on the films. The two-step method provided a higher amount of PbI_2 regarding the reaction of methyl ammonium iodide (MAI) with an outer layer of the first bonded PbI_2 hindered the inner layer to interact with MAI. The Ostwald ripening (OR) process that was applied to the thin film resulted through one-step deposition synthesis has successfully converted the unformed PbI_2 to $MAPbI_3$ with a more uniform, lower void, and higher crystal size as confirmed by XRD and SEM analysis results. The application of $MAPbI_3$ prepared using OR treatment in the solar cell resulted in higher efficiency (7.64%) than the one synthesized without OR (4.91%).
Keywords: Ostwald ripening, $CH_3NH_3PbI_3$, Perovskite Solar Cell, Organometallic halide
RASĀYAN *J. Chem.*, Vol. 15, No.3, 2022

INTRODUCTION

The development of solar cell technology based on organic-inorganic hybrid perovskite has attracted much attention since it demonstrated exceptional progress in solar cell performance[1–3] and its low-cost preparation methods.[4,5] Since the first reported perovskite-based solar cell (PSC) in 2009 with an efficiency of 3.8%[1], the current PSC devices have significantly developed achieving an efficiency above 22%.[6] The remarkable efficiency of PSC is highly affected by the perovskite's multitude of properties, especially the combination of good optical absorption characteristics with efficient-charge transport properties[7], broad and balance of charge diffusion[8], and a good bipolar carrier.[9] Furthermore, PSC is more environmentally friendly and has faster energy payback times compared to silicon-based solar cell[4], making it a potential candidate for renewable energy technology. The methylammonium lead iodide ($CH_3NH_3PbI_3$, $MAPbI_3$) perovskite was widely reported as the most highly effective material as a light harvester and electron generator in the PSC system.[10–13] Several synthesis approaches and methods have been reported by many researchers to obtain a high-quality $MAPbI_3$ film, such as one- or two-step the process in solution[13–17], solid-state process[18], and vapor process.[19] The one-step spin-coating has become the most popular simple method for the solution performing crystallization-engineered perovskite films.[17,20] A high uniformity and less crystal defect perovskite films were obtained by applying an antisolvent on the films under spinning during the coating process to provide a fast process of nucleation and crystallization.[21] In a one-step deposition, a precursor containing MAX and PbX_2 (X= Br dan/atau I) in N,N-dimethylformamide (DMF) or isopropanol was coated and calcined to obtain $MAPbX_3$ through two main processes that occur simultaneously, i.e. excessive solvent evaporation and perovskite crystallization.[20] However, the one-step method is quite difficult to produce a homogeny and free-defect perovskite thin film and the application of the one-step prepared material in the PSC system might lead to the stability problems of the device.

The two-step spin coating process has been widely used since it provided a better method to control the perovskite crystal and morphology by varying the composition.[5,22–24] In the two-step process, the $MAPbI_3$ was formed through first, the deposition of the PbI_2 layer on the semiconductor film by dipping or spin-

http://doi.org/10.31788/RJC.2022.1536890

coating, and second, the perovskite conversion process, in which a solution containing methyl ammonium iodide (MAI) is introduced to the PbI_2 seed above the semiconductor layer.[25,26] The perovskite formation generally involves complex processes, a short time, and a specific atmosphere which is highly responsible for the problem of reproducibility and the specific advanced laboratory. The fast process of crystallization leads to the formation of low uniformity of nanocrystal size and a high percentage of crystal defect[19,21], while the atmosphere of the deposition process is highly influencing the perovskite film quality. Some post-treatment techniques have been applied to reduce the crystal defect formation and enlarge the crystal size, such as solvent engineering and a specific annealing process. However, these treatments also required some specific atmosphere and sophisticated techniques that are difficult to obtain under ambient conditions. Therefore, it is a need to develop a facile technique to synthesize a uniform perovskite crystal with a low defect that can be done under ambient conditions. Ostwald ripening is the potential simplest method to refine the small crystals into large ones via a thermodynamically spontaneous process. Here, we report the one and two-step synthesis of methyl ammonium lead triiodide ($MAPbI_3$) followed by Ostwald ripening post-treatment under ambient conditions.

EXPERIMENTAL

TiO_2 Thin Film Preparation

Fluorine-doped tin-oxide (FTO) contained glass substrates (Solaronic) were edged using Zinc powder and 0.2 M HCl; sequentially cleaned in an ultrasonic bath with isopropanol, acetone, and de-ionized water. Compact titanium dioxide (c-TiO_2) was formed by adding the homogenous solution of 0.46 ml of titanium tetraisopropoxide (TTIP) in 5 ml ethanol on FTO substrates under spinning at 4000 rpm for the 30s and sintered at 500 ^oC for 30 minutes in the ambient environment. The synthesis of mesoporous TiO_2 (m-TiO_2) was done following the previously developed procedure with slight modification.[27] The deposition of the m-TiO_2 layer was done by spin coating of the m-TiO_2 paste in ethanol (2/7 (w/w)) on previous FTO/c-TiO_2 film at 4000 rpm for 30 s and annealed at 500 ^oC for 30 minutes.

Perovskite Film Preparation

The perovskite material was prepared through the one-step and two-step coating methods. The one-step spin coating method was applied by adding the mixture of MAI and PbI_2 to the prepared FTO/TiO_2 thin film under spinning at 4000 rpm for 40 s and heated at 150 ^oC for 5 min on the hotplate. The two-step method was performed as followed: PbI_2 layer was firstly deposited on the FTO/TiO_2 film by spin coating a 1 M solution of PbI_2 in DMF at 4000 rpm for 40 s and dried at 150 ^oC for 15 min on a hot plate. Specific concentrations of MAI solution in DMF (30mg/ml) were then added to the PbI_2 seed layer and spin-coated at 4000 rpm for 40 s and heated at 150 ^oC for 5 min to complete the formation of $MAPbI_3$.The Ostwald ripening process was initiated by dropping 0.5 ml of diethyl ether before applying the MAI solution (30 mg/ml) to the FTO/TiO_2/$MAPbI_3$ thin films resulting from one-step methods. All processes were done under ambient conditions at room temperature and humidity. The structure of resulted films was studied using XRD (Rigaku 1000). Morphology of perovskite thin films was studied using SEM (Hitachi) and the electronic structure was analyzed using UV-Vis Spectrophotometer (UV-2600, Shimadzu).

Solar Cell Fabrication and Characterization

The PSC device was fabricated using previously synthesized FTO/c-TiO_2/m-TiO_2/$MaPbI_3$ as an electron generating electrode. Spiro-OMeTAD (2,2',7,7'-Tetrakis(N,N-di-p-methoxyphenylamino)-9,9'-spirobifluorene) mixed with Li-TFSI and 4-TBP were used as Hole Transporting Layer (HTL) and spin-coated on FTO/c-TiO_2/m-TiO_2/$MaPbI_3$ film at 2500 rpm for the 30s. Au layer as the counter electrode was deposited on the HTL layer by thermal evaporation. The devices were then fixed using an aluminum mask. The I-V characteristic of the PSC was measured by Keithley 2400 instrument under 100 mW/cm^2 (AM 1.5 sun radiation).

RESULTS AND DISCUSSION

The XRD analysis was used to study the structural properties of materials formed during the synthesis process. c-TiO_2 was the first layer deposited on conducting glass to form FTO/c-TiO_2 thin film. The XRD analysis results of FTO/c-TiO_2 with the Le Bail refinement using the Rietica program (Fig.-1a) showed

that there are three TiO_2 crystal phases found in the film. Two diffraction peaks at 2θ = 38° and 62° are relating to the (011) and (121) crystal planes of anatase TiO_2 (COD No. 96-900-8217), peak at 2θ = 27° is indicating the (110) crystal plane of rutile TiO_2 (COD No. 96-900-4145), and peaks at 2θ = 34°, 52°, and 65° are confirming to brookite crystal planes (COD No.96-900-4140). The crystal parameters refined by the Le Bail method using the Rietica program are listed in Table-1, which showed that anatase and brookite are the dominant crystal phases. Mesoporous TiO_2 (m-TiO_2) was prepared through the sol-gel method using dodecylamine as a pore template. The resulting m-TiO_2 was then applied to the FTO/c-TiO_2 to obtain FTO/c-TiO_2/m-TiO_2 thin film. The XRD result of FTO/c-TiO_2/m-TiO_2 (Fig.-1b) showed that there are only two TiO_2 crystal phases found in the film, namely anatase, and rutile. The refinement result of FTO/c-TiO_2/m-TiO_2 is listed in Table-2, which showed that the anatase crystal phase is the main resulting crystal phase (~81% molar percentage) and there is no brookite phase found. The annealing process at 500°C is not thermodynamically suitable yet to transform anatase become a rutile crystal phase, as already expected according to a previous study reported.[28] These result means that the mesoporous layer of m-TiO_2 could perfectly cover the c-TiO_2 to provide a layer as electron transporting material (ETM), as support of the perovskite material, and to avoid the morphology defect of perovskite solar cell.

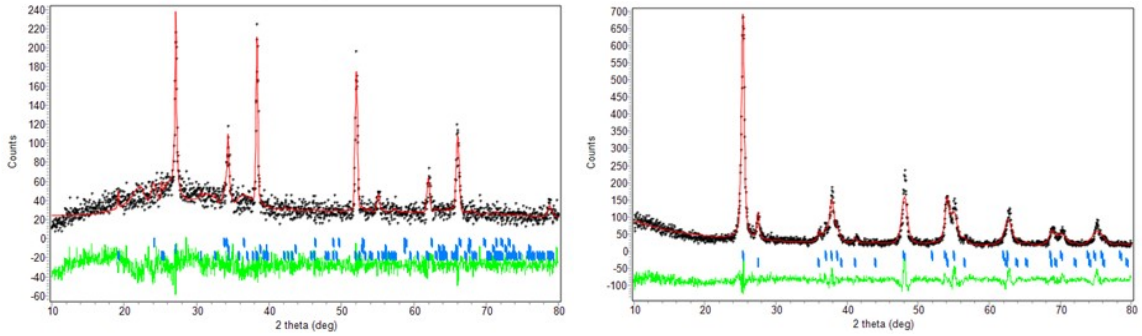

a b

Fig.-1: XRD Analysis and the Le Bail Refinement Results of a. FTO/c-TiO_2 and b. FTO/c-TiO_2/m-TiO_2

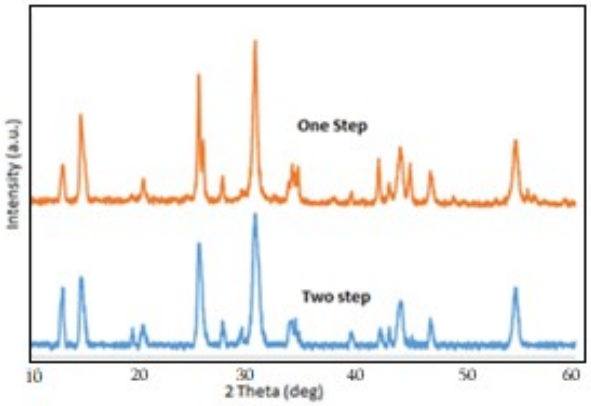

Fig.-2: XRD Analysis Result of FTO/TiO_2/$MAPbI_3$ Prepared by One- and Two-Step Methods

Table-1: Lattice Parameters and Crystal Volume of c-TiO_2

Parameter	Compact-TiO_2					
	COD no. 96-900-8217	Fasa 1 TiO_2 Anatase	COD no. 96-900-4145	Fasa 2 TiO_2 Rutile	COD no. 96-900-4140	Fasa 3 TiO_2 Brookite
Crystal system	Tetragonal	Tetragonal	Tetragonal	Tetragonal	Orthorhombic	Orthorhombic
Space Group	I 41/A M D	I 41/A M D	P 42/M N M	P 42/M N M	P B C A	P B C A
a (Å)	3.80400	3.9057	4.62300	4.6245	9.19100	9.1559
b (Å)	3.80400	3.9057	4.62300	4.6245	5.46300	5.4675
c (Å)	9.61400	10.5557	2.98600	3.1389	5.15700	5.1849
α (°) = β (°) = γ (°)	90	90	90	90	90	90

Cell Volume (Å^3)	139.1186	161.021881	63.8172	67.128502	258.9352	259.555511
Bragg Factor	-	0.02	-	0.01	-	0.02
Gof (x^2)	-	0.0798	-	0.0798	-	0.0798
Rp (%)	-	14.46	-	14.46	-	14.46
Rwp (%)	-	20.08	-	20.08	-	20.08
Phase Molar (%)	-	49.64	-	10.35	-	40.01

Table-2: Lattice Parameters and Crystal Volume of m-TiO_2

Parameter	Compact-TiO_2			
	COD no. 96-900-8217	Fasa 1 TiO_2 Anatase	COD no. 96-900-4145	Fasa 2 TiO_2 Rutile
Crystal system	Tetragonal	Tetragonal	Tetragonal	Tetragonal
Space Group	I 41/A M D	I 41/A M D	P 42/M N M	P 42/M N M
a (Å)	3.80400	3.8040	4.62300	4.6229
b (Å)	3.80400	3.8040	4.62300	4.6229
c (Å)	9.61400	9.5655	2.98600	2.9860
α (°) = β (°) = γ (°)	90	90	90	90
Cell Volume (Å^3)	139.1186	138.416763	63.8172	63.814419
Bragg Factor	-	0.01	-	0.01
Gof (x^2)	-	0.1484	-	0.1484
Rp (%)	-	13.70	-	13.70
Rwp (%)	-	12.71	-	12.71
Phase Molar (%)	-	81.27	-	18.73

The formation of $MAPbI_3$ on the TiO_2 layer was done through one- and two-steps method before applying Ostwald ripening to study the mechanism of perovskite formation. The XRD results of perovskite on TiO_2 are shown in Fig.-2, which indicated the appearance of $MAPbI_3$ in both results. The perovskite crystal was confirmed by sharp peaks at 2θ of 14.4°, 20.4°, 24.9°, 28.5° 32.4°, and 32.3°, which in the range of $MAPbI_3$ correspond to (002), (112), (022), (004), (222), and (104) planes.[24,25,28] The characteristic of PbI_2 peaks were still found in both XRD results, which is indicating that the perovskite formation was incomplete through a one-or two-step method. This is a common result from the $MAPbI_3$ perovskite synthesis, even if it is conducted under specific humidity and the unformed PbI_2 could influence the overall solar cell efficiency by hindering the electron diffusion from the perovskite to the ETM layer. However, the two-step coating method resulted in a higher PbI_2 dominant peak intensity (2θ of 12.7° and 18.9°). In the one-step method, the PbI_2 could react with MAI in the solution to result in $MAPbI_3$ perovskite even before it is applied on the TiO_2 surface, while in the two-step method, the first bonded PbI_2 let mostly only the outer layer to interact with MAI resulted in a dense $MAPbI_3$ layer and blocking the inner PbI_2 layer to react with MAI which leads to a higher amount of unformed PbI_2 (Fig.-3).

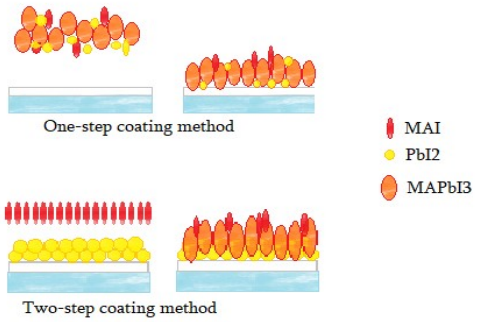

Fig.-3: Mechanism Scheme of one- and two-Step Method of $MAPbI_3$ Perovskite Synthesis

The electronic properties of resulted $MAPbI_3$ perovskite on TiO_2 thin films synthesized by one- and two-step methods were analyzed using UV Vis Spectrophotometer as shown in Fig.-4. It was shown that the

$MAPbI_3$ synthesized through the one-step method provides a significantly higher intensity in the visible light region, which might be contributed by a higher amount of $MAPbI_3$ as a light-absorbing layer. Since perovskite also plays an important role as an electron/hole transport layer, the higher concentration of perovskite leads to a more effective charge diffusion as a starting generation of electricity. Therefore, we applied the Ostwald ripening post-treatment to the perovskite synthesized through the one-step spin coating method. Furthermore, the unformed PbI_2 on the film prepared through a two-step method was covered by the $MAPbI_3$ layer, the additional reaction with MAI is retarded since the diffusion of MAI is rather difficult through the $MAPbI_3$ layer.[29]

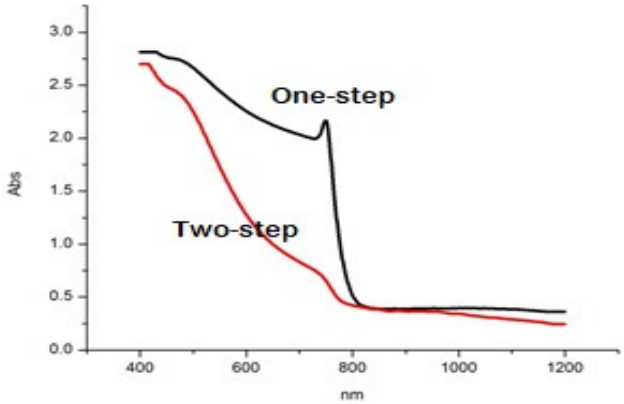

Fig.-4: UV-Vis Spectra of N-TiO_2 Synthesized with and without reflux

The application of Ostwald ripening treatment to FTO/TiO_2/$MAPbI_3$ thin film synthesized through one-step method could successfully convert the unformed PbI_2 to $MAPbI_3$, as confirmed by XRD analysis results (Fig.-5). There are no PbI_2 characteristic peaks left on the treated thin film and only sharp peaks of $MAPbI_3$ characteristics appeared on the diffractogram. Thus, the Ostwald ripening process increases the perovskite's crystallinity and uniformity and also resulted in a higher size of perovskite calculated by the Scherrer formula as listed in Table-3. The Ostwald ripening process indeed dissolved the smaller crystal of perovskite which then deposited as a larger crystal or particle.[30,31]

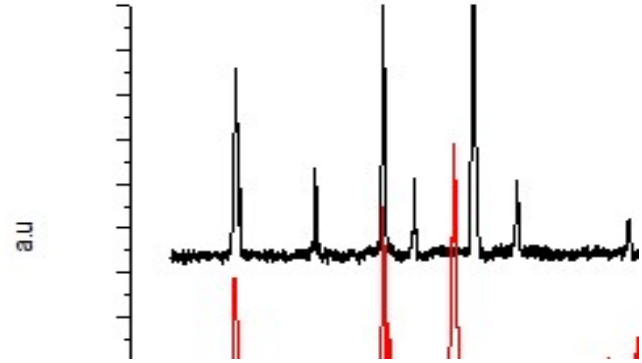

Fig.-5: XRD Analysis Results of FTO/TiO_2/$MAPbI_3$ without and with Ostwald Ripening Process

Table-3: Characteristics of $CH_3NH_3PbI_3$ Crystal Based on XRD

Angle	hkl	Size no OR (±10 nm)	Size with OR (±10 nm)
14.5	002, 110	96	168
20.4	112,020	180	310
25.0	022	126	335
28.8	004, 220	161	322
32.3	114, 222,130	118	274
35.4	024, 132	128	260

The morphology of perovskite analyzed using SEM (Fig.-6) has confirmed the result of XRD. It showed that the Ostwald ripening treatment resulted in a more uniform, less pinhole, and higher crystal of perovskite. The existence of a pinhole in the perovskite layer indicates the quality of $MAPbI_3$ thin film even after applying the Ostwald ripening process, which is highly related to the uncontrolled humidity. Wozny *et al.* reported the influence of humidity in the synthesis of formamidinium lead-triiodide perovskite, the higher humidity resulted in a more non-homogenous film consisting of many pinholes, a film crystallinity reduction, and a decay of optical properties.[32] The application of prepared $FTO/TiO_2/CH_3NH_3PbI_3$ from a one-step spin-coating deposition process with and without Ostwald ripening (Fig.-7) showed that the OR post-treatment applied during the synthesis has resulted in higher efficiency than the one without OR.

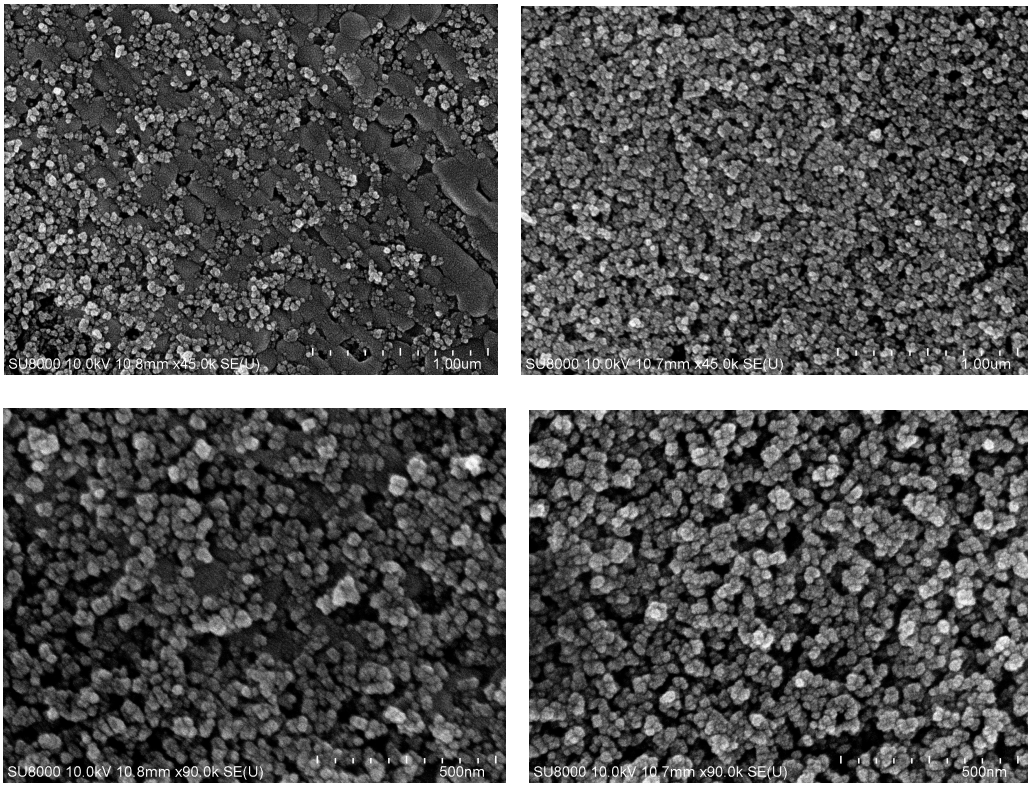

a b

Fig.-6: SEM Micrographs of $FTO/TiO_2/MAPbI_2$ Prepared without (a) and with (b) Ostwald Ripening at Magnificent of 4500x (up) and 90000x (down)

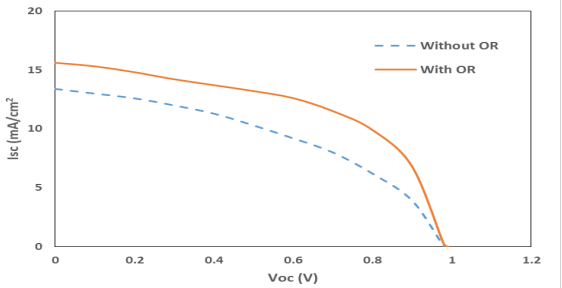

Fig.-7: I-V Curve of PSC Based on Prepared $FTO/TiO_2/MAPbI_3$

Table-4: Characteristics of PSC Based on Prepared $FTO/TiO_2/MAPbI_3$

$FTO/TiO_2/MAPbI_3$	I_{SC} (mA/cm^2)	V_{OC} (V)	FF (%)	PCE (%)
No OR	12.4	0.98	40.40	4.91
With OR	15.6	0.99	49.44	7.64

CONCLUSION

The methyl ammonium lead iodide ($CH_3NH_3PbI_3$) have been successfully synthesized under ambient condition using the one-step spin-coating deposition method continued by Ostwald ripening. The Ostwald ripening as a post-treatment has completely converted the unformed PbI_2 left on the resulted film to $MAPbI_3$ and resulted in a more uniform, less pinhole, and larger perovskite crystal. The Ostwald ripening process that was applied during the synthesis also resulted in a better active layer for a solar cell application, leading to a higher conversion efficiency compared to the perovskite prepared without Ostwald ripening.

ACKNOWLEDGMENT

Financial support from the Indonesian Government granted by Universitas Negeri Yogyakarta through Program Percepatan Guru Besar Tahun 2021 is gratefully acknowledged.

REFERENCES

1. A. Kojima, K. Teshima, Y. Shirai and T. Miyasaka, *Journal of American Chemical Society,* **131**, 6050(2009), http://doi.org/10.1021/ja809598r
2. Z. Song, S.C. Watthage, A.B. Phillips, and M.J. Heben, *Journal of Photonics Energy,* **6**, 022001 (2016), http://doi.org/10.1117/1.JPE.6.022001
3. R. Liu, *Materials (Basel)* **7**, 2747(2014), http://doi.org/10.3390/ma7042747
4. I. Celik, Z. Song, A.J. Cimaroli, Y. Yaj, M.J. Heben, and D. Apul, *Solar Energy Material and Solar Cells,* **156**, 157(2016), http://doi.org/10.1016/j.solmat.2016.04.037
5. J. Burschka, N. Pellet, S-J Moon, R. Humphry-Baker, P. Gao, M.K. Nazeeruddin & M. Gratzel, *Nature,* **499**, 316(2013), http://doi.org/10.1038/nature12340
6. H. Zhou, Q. Chen, G. Li, S. Luo, T-B Song, H-S Duan, Z. Hong, J. You, Y. Liu, and Y. Yang, *Science,* **345(6196)**, 542(2014), http://doi.org/10.1126/science.1254050
7. C.C. Vidyasagar, B.M. Muñoz Flores, and V.M. Jiménez Pérez, *Nano-Micro Letters,* **10**, 448(2018), http://doi.org/10.1007/s40820-018-02221-5
8. G. Xing, N. Matews, S. Sun, S.S. Lim, Y.M. Lam, M. Gratzel, S. Maisalkhar, and T.C. Sum, *Science,* **80**, 342(2013), http://doi.org/10.1126/science.1243167
9. M.H. Hoang, Y. Kim, M. Kim, K.H. Kim, T.W. Lee, D.N. Nguyen, S-J Kim, K. Lee, S.J. Lee, D.H. Choi, *Advanced Materials,* **24**, 5363(2012), http://doi.org/10.1002/adma.20120214
10. M.A. Green and A. Ho-Baillie, *ACS Energy Letters,* **2**, 822(2017), http://doi.org/10.1021/acsenergylett.7b00137
11. H.J. Snaith, *Journal of Physical Chemistry Letter,* **4**, 3623(2013), http://doi.org/10.1021/jz4020162
12. S.C. Watthage, Z. Song, G.K. Liyanage, A. B. Phillips, and M.J. Heben, *Conf. Rec. IEEE Photovoltaic Specific Conf.,* **2016-Novem**, 831(2016), http://doi.org/10.1109/PVSC.2016.7749723
13. Y. Zhang, Z. Fei, P. Gao, Y. Lee, F.F. Tirani, R. Scopelliti, Y. Feng, P.J. Dyson, M.K. Nazeeruddin, *Advanced Materials,* **29**, (2017), http://doi.org/10.1002/adma.201702157
14. J.H. Im, H.S. Kim, and N.G. Park, *APL Material,* **2**, (2014), http://doi.org/10.1063/1.4891275
15. L. Zheng, D. Zhang, Y. Ma, Z. Lu, Z. Chen, S. Wang, L. Xiao, and Q. Gong, *Dalton Transaction,* **44**, 10582(2015), http://doi.org/10.1039/C4DT03869J
16. N. Ahn, D.Y. Son, I.H. Jang, S.M. Kang, M. Choi, and N.G. Park, *Journal of American Chemical Society,* **137**, 8696(2015), http://doi.org/10.1021/jacs.5b04930
17. N.J. Jeon, J.H. Noh, Y.C. Kim, W.S. Yang, S. Ryu, and S.I. Seok, *Nature Materials,* **13**, 897(2014), http://doi.org/10.1038/nmat4014
18. Y. Zhou, M. Yang, A.L. Vasiliev, H.F. Garces, Y. Zhao, D. Wang, S. Pang, K. Zhu, N.P. Padture, *Journal of Material Chemistry,* **A 3**, 9249(2015), http://doi.org/10.1039/C4T407036D
19. M. Xiao, F. Huang, W. Huang, Y. Dkhissi, Y. Zhu, J. Etheridge, A. Gray-Weale, U. Bach, Y.B. Cheng, L. Spiccia, *Angewandte Chemie-International Edition,* **53**, 9898(2014), http://doi.org/10.1002/anie.201405334
20. W. Zhu, C. Bao, Y. Wang, F. Li, X. Zhou, J. Yang, B. Lv, X. Wang, T. Yu, and Z. Zou, *Dalton Transaction,* **45**, 7856(2016), http://doi.org/10.1039/c6dt00900j
21. E.D. Gaspera, Y. Peng, Q. Hou, L. Spiccia, U. Bach, J.J. Jasieniak, Y.B. Cheng, *Nano Energy,* **13**,

249(2015), http://doi.org/10.1016/j. nanoen.2015.02.028
22. N.J. Jeon, J.H. Noh, W.S. Yang, Y.C. Kim, S. Ryu, J. Seo, and S.I. Seok, *Nature,* **517**, 476(2015), http://doi.org/10.1038/nature14133
23. W. Chen, Y. Wu, Y. Yue, J. Liu, W. Zhang, X. Yang, H. Chen, E. Bi, I. Ashraful, M. Gratzel, and L. Han, *Science,* **350(6263)**, 944(2015), http://doi.org/10.1126/science.aad1015
24. A. Mei, X. Li, L. Liu, Z. Ku, T. Liu, Y. Rong, M. Xu, M. Hu, J. Chen, Y. Yang, M. Gratzel, and H. Han, *Science,* **345(6194)**, 295(2014), http://doi.org/10.1126/science.1254763
25. Y.J. Jeon, S. Lee, R, Kang, J.E. Kim, J.S. Yeo, S.H. Lee, S.S. Kim, J.M. Yun, & D.Y. Kim, *Science, Republic* **4**, 26(2014), http://doi.org/10.1038/srep06953
26. C. Kusumawardani, *Rasayan Journal of Chemistry,* **15(1)**, 549(2022), http://doi.org/10.31788/RJC.2022.1516674
27. C. Kusumawardani, K.H. Sugiyarto, A.K. Prodjosantoso, *Molekul,* **16(3)**, 268(2021), http://doi.org/10.20884/1.jm.2021.16.3.804
28. J.H. Im, I.H. Jang, N. Pellet, M.Grätzel, and N.G. Park, *Nature Nanotechnology,* **9**, 927(2014), http://doi.org/10.1038/nnano.2014.181
29. S.Y. Kim, H.J. Jo, S.J. Sung, and D.H. Kim, *APL Material,* **4**, (2016), http://doi.org/10.1063/1.4963841
30. A. Ren, H. Lai, X. Hao, Z. Tang, H. Xu, B.M.F.Y. Jeco, K. Watanabe, L. Wu, J. Zhang, M. Sugiyama, J. Wu, D. Zhao, *Joule,* **4**, 1263(2020), http://doi.org/10.1016/j.joule.2020.04.013
31. M. Yang, T. Zhang, P. Schulz, Z. Li, G. Li, D.H. Kim, N. Guo, J.J. Berry, K. Zhu, & Y. Zhao, *Nature Communication,* **7**, 2(2016), http://doi.org/10.1038/ncomms12305
32. S. Wozny, M. Yang, A.M. Nardes, C.C. Mercado, S. Ferrere, M.O. Reese, W. Zhou, and K. Zhu, *Chemistry of Materials,* **27**, 4814(2015), http://doi.org/10.1021/acs.chemmater.5b01691

[RJC-6890/2021]